



ACADEMIC  
PRESS

Available online at [www.sciencedirect.com](http://www.sciencedirect.com)

SCIENCE @ DIRECT®

Journal of Sound and Vibration 267 (2003) 355–365

JOURNAL OF  
SOUND AND  
VIBRATION

[www.elsevier.com/locate/jsvi](http://www.elsevier.com/locate/jsvi)

Letter to the Editor

# On the eigencharacteristics of multi-step rods carrying a tip mass subjected to non-homogeneous external viscous damping

M. Gürgöze\*, H. Erol

*Faculty of Mechanical Engineering, Technical University of Istanbul, 80191 Gümüüşsuyu, Istanbul, Turkey*

Received 8 October 2002; accepted 9 January 2003

## 1. Introduction

Recently, an interesting study [1] was published in this journal and in that study the eigencharacteristics of a continuous beam model with damping was determined using the separation of variables approach. The beam considered has different physical properties in each of its two parts. Motivated by that publication, in Ref. [2], the present authors dealt with an axially vibrating rod consisting of two parts as a counterpart of that publication. Unlike Ref. [1], where overdamped and underdamped “modes” are investigated separately, both of them were handled simultaneously in Ref. [2], again via separation of variables approach. The present study is more general than the previous work because the rod system considered here consists of several different parts. Besides, a second method is given for the determination of the eigencharacteristics, and this method also used the separation of the variables approach. The reason the second method is given is its use in testing the reliability of the first method, besides perhaps being numerically more advantageous in the case of a large number of rod steps. Probable applications of these rod systems include rods composed of several different cross-sections with different dampings subject to impulsive axial forces in civil engineering applications. Such systems can also be encountered in oil well drilling practices.

## 2. Theory

Let us assume that an axially vibrating rod carrying a tip mass  $M$  consists of  $n$  parts, the  $i$ th of which has the length  $L_i$ , axial rigidity  $E_i A_i$ , viscous damping coefficient  $c_i$ , and mass per unit length  $m_i$ . These parameters are assumed to be constant along each rod segment, and contain contributions from the rod and any surrounding medium. Fig. 1 shows the rod diagrammatically.

\*Corresponding author. Fax: +90-212-245-07-95.

*E-mail address:* [gurgozem@itu.edu.tr](mailto:gurgozem@itu.edu.tr) (M. Gürgöze).

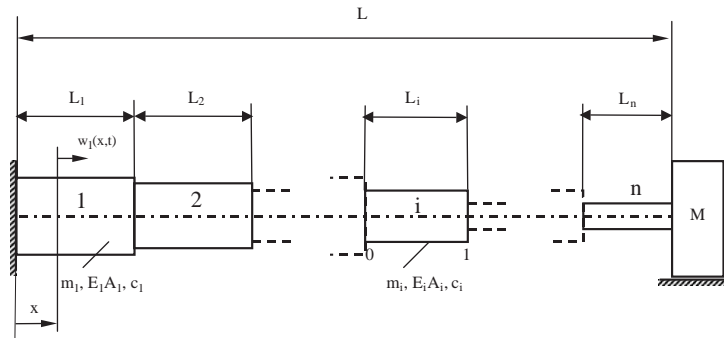


Fig. 1. Axially vibrating elastic rod having several parts and carrying a tip mass.

Due to the presence of external viscous damping, it is more appropriate to work with complex variables. It will be assumed that the axial displacements  $w_i(x, t)$  ( $i = 1, \dots, n$ ) of several parts of the rod are the real parts of some complex quantities denoted  $z_i(x, t)$ . Keeping in mind that actually, one is interested only in the real parts of the expressions below, the equations of motion of the rod can be written as

$$k_i z_i''(x, t) - m_i \ddot{z}_i(x, t) - c_i \dot{z}_i(x, t) = 0 \quad (i = 1, \dots, n) \tag{1}$$

with  $k_i = E_i A_i$ , where  $x$  is the axial position along the rod. Dots and primes denote partial derivatives with respect to time  $t$  and position co-ordinate  $x$ , respectively.

The corresponding boundary conditions are

$$\begin{aligned} z_1(0, t) &= 0, \\ z_{i-1}(\bar{L}_i, t) &= z_i(\bar{L}_i, t), \quad k_{i-1} z'_{i-1}(\bar{L}_i, t) = k_i z'_i(\bar{L}_i, t) \quad (i = 2, \dots, n), \\ k_n z'_n(L, t) + M \ddot{z}_n(L, t) &= 0, \end{aligned} \tag{2}$$

where

$$\bar{L}_i = \sum_{j=1}^{i-1} L_j, \quad L = \sum_{j=1}^n L_j. \tag{3}$$

Let us assume that

$$z_i(x, t) = Z_i(x) D_i(t) \quad (i = 1, \dots, n) \tag{4}$$

according to the separation of the variables approach, where both functions  $Z_i(x)$  and  $D_i(t)$  are complex functions in general. Substituting Eq. (4) into Eq. (1) gives

$$\frac{k_i Z_i''(x)}{m_i Z_i(x)} = \frac{\ddot{D}_i(t) + (c_i/m_i) \dot{D}_i(t)}{D_i(t)} := \kappa_i, \tag{5}$$

where the  $\kappa_i$  are complex constants to be determined. Here, primes and dots denote derivatives with respect to position  $x$  and time  $t$ , respectively. To satisfy the “second” and “third” of the boundary conditions (2), the corresponding time functions must be equal, so that  $D_i(t) = D(t)$

( $i = 1, \dots, n$ ). Thus, the differential equations for  $Z_i(x)$  may be written using Eq. (5) as follows:

$$Z_i''(x) - \frac{m_i}{k_i} \kappa_i Z_i(x) = 0 \quad (i = 1, \dots, n). \tag{6}$$

The time function is assumed now an exponential function:

$$D(t) = e^{\lambda t}, \tag{7}$$

where  $\lambda$  represents an eigenvalue of the system which is complex in general. With this  $D(t)$ , the second equality in (5) gives

$$\kappa_i = \frac{c_i}{m_i} \lambda + \lambda^2 \quad (i = 1, \dots, n). \tag{8}$$

Defining

$$v_i^2 = \frac{m_i}{k_i} \kappa_i \quad (i = 1, \dots, n) \tag{9}$$

the first equation in (5) can be written as

$$Z_i''(x) - v_i^2 Z_i(x) = 0 \quad (i = 1, \dots, n). \tag{10}$$

The general solutions of the differential equation (10) can be expressed as

$$Z_i(x) = \bar{A}_i e^{v_i x} + \bar{B}_i e^{-v_i x} \quad (i = 1, \dots, n), \tag{11}$$

where  $\bar{A}_i$  and  $\bar{B}_i$  denote complex constants to be determined. In terms of the  $Z_i(x)$ , and with the aid of Eq. (7), the boundary conditions in (2) can be reformulated:

$$Z_1(0) = 0,$$

$$Z_{i-1}(\bar{L}_i) = Z_i(\bar{L}_i), \quad k_{i-1} Z'_{i-1}(\bar{L}_i) = k_i Z'_i(\bar{L}_i) \quad (i = 2, \dots, n),$$

$$k_n Z'_n(L) + M \lambda^2 Z_n(L) = 0. \tag{12}$$

The substitution of expressions (11) into (12) yields the following set of  $2n$  homogeneous equations for the determination of the  $2n$  unknowns  $\bar{A}_i, \bar{B}_i$  ( $i = 1, \dots, n$ ):

$$\begin{bmatrix} 1 & 1 & 0 & 0 & 0 & 0 & \dots & 0 & 0 \\ e^{v_1 \bar{L}_2} & e^{-v_1 \bar{L}_2} & -e^{v_2 \bar{L}_2} & -e^{-v_2 \bar{L}_2} & 0 & 0 & \dots & 0 & 0 \\ k_1 v_1 e^{v_1 \bar{L}_2} & -k_1 v_1 e^{-v_1 \bar{L}_2} & -k_2 v_2 e^{v_2 \bar{L}_2} & k_2 v_2 e^{-v_2 \bar{L}_2} & 0 & 0 & \dots & 0 & 0 \\ 0 & 0 & e^{v_2 \bar{L}_3} & e^{-v_2 \bar{L}_3} & -e^{v_3 \bar{L}_3} & -e^{-v_3 \bar{L}_3} & \dots & 0 & 0 \\ 0 & 0 & k_2 v_2 e^{v_2 \bar{L}_3} & -k_2 v_2 e^{-v_2 \bar{L}_3} & -k_3 v_3 e^{v_3 \bar{L}_3} & k_3 v_3 e^{-v_3 \bar{L}_3} & \dots & 0 & 0 \\ 0 & 0 & 0 & 0 & e^{v_3 \bar{L}_4} & e^{-v_3 \bar{L}_4} & \dots & 0 & 0 \\ 0 & 0 & 0 & 0 & k_3 v_3 e^{v_3 \bar{L}_4} & -k_3 v_3 e^{-v_3 \bar{L}_4} & \dots & 0 & 0 \\ \vdots & \vdots & \vdots & \vdots & \vdots & \vdots & \vdots & \vdots & \vdots \\ 0 & 0 & 0 & 0 & 0 & 0 & \dots & -k_{n-1} v_{n-1} e^{v_{n-1} \bar{L}_{n-1}} & k_{n-1} v_{n-1} e^{-v_{n-1} \bar{L}_{n-1}} \\ 0 & 0 & 0 & 0 & 0 & 0 & \dots & (k_n v_n + M \lambda^2) e^{v_n L} & -(k_n v_n - M \lambda^2) e^{-v_n L} \end{bmatrix} \begin{bmatrix} \bar{A}_1 \\ \bar{B}_1 \\ \bar{A}_2 \\ \bar{B}_2 \\ \bar{A}_3 \\ \bar{B}_3 \\ \bar{A}_4 \\ \bar{B}_4 \\ \vdots \\ \bar{A}_n \\ \bar{B}_n \end{bmatrix} = 0. \tag{13}$$

Let the  $(2n \times 2n)$  matrix of coefficients in Eq. (13) be denoted by  $\mathbf{A}$ . For a non-trivial solution, the determinant of this matrix should be zero:

$$\det \mathbf{A}(v_1, \dots, v_n) = 0. \tag{14}$$

If in Eq. (14) the tip mass  $M$  approaches infinity, then the characteristic equation of the axially vibrating rod fixed at both ends is obtained, which is given in Ref. [2] for  $n=2$ . Equating to zero the tip mass  $M$  yields the characteristic equation of the fixed-free rod.

Using the definitions given by (8) and (9),  $v_i$  ( $i = 1, \dots, n$ ) can be expressed as functions of the eigenvalue  $\lambda$ :

$$v_i(\lambda) = \pm \sqrt{\frac{m_i}{k_i} \left[ \left( \frac{c_i}{m_i} \right) \lambda + \lambda^2 \right]} \quad (i = 1, \dots, n). \tag{15}$$

Hence, Eq. (14) becomes

$$\det \mathbf{A}(v_1(\lambda), \dots, v_n(\lambda)) = \det \mathbf{A}(\lambda) = 0 \tag{16}$$

from which  $\lambda$  can be obtained, which is a complex number in general. Now via (15) the  $v_i$ 's can be obtained. If these are substituted into the coefficients matrix  $\mathbf{A}$  in Eq. (13), the unknowns  $\bar{A}_i, \bar{B}_i$  ( $i = 1, \dots, n$ ) can be determined up to an arbitrary constant. Hence,  $Z_i(x)$ , ( $i = 1, \dots, n$ ) in Eq. (11) are obtained.

Returning to Eq. (4) and considering expression (11) and introducing

$$\lambda = \lambda_{re} + j\lambda_{im}, \quad v_i = v_{ire} + jv_{iim},$$

$$\bar{A}_i = \bar{A}_{ire} + j\bar{A}_{iim}, \quad \bar{B}_i = \bar{B}_{ire} + j\bar{B}_{iim} \quad (j = \sqrt{-1}), \tag{17}$$

the axial displacements of the  $n$  portions of the rod,  $w_i(x, t)$ , are determined, after lengthy calculations, as

$$w_i(x, t) = \text{Re} [z_i(x, t)] = e^{\lambda_{re}t} S_i(x) \cos \lambda_{im}t - e^{\lambda_{re}t} Q_i(x) \sin \lambda_{im}t, \tag{18}$$

where the following abbreviations are introduced:

$$\begin{aligned} S_i(x) &= e^{v_{ire}x} (\bar{A}_{ire} \cos v_{iim}x - \bar{A}_{iim} \sin v_{iim}x) + e^{-v_{ire}x} (\bar{B}_{ire} \cos v_{iim}x + \bar{B}_{iim} \sin v_{iim}x), \\ Q_i(x) &= e^{v_{ire}x} (\bar{A}_{ire} \sin v_{iim}x + \bar{A}_{iim} \cos v_{iim}x) + e^{-v_{ire}x} (\bar{B}_{iim} \cos v_{iim}x - \bar{B}_{ire} \sin v_{iim}x). \end{aligned} \tag{19}$$

The expressions of the axial displacements can be put in a more compact form as

$$w_i(x, t) = e^{\lambda_{re}t} C_i(x) \cos (\lambda_{im}t - \varepsilon_i(x)) \tag{20}$$

with

$$C_i(x) = \sqrt{S_i^2(x) + Q_i^2(x)}, \quad \tan \varepsilon_i(x) = -\frac{Q_i(x)}{S_i(x)}. \tag{21}$$

$w_i(x, t)$  ( $i = 1, \dots, n$ ) determine the axial displacement distribution over the length of the viscously damped rod when it vibrates at an eigenvalue  $\lambda$ . Due to the apparent presence of a phase which is a function of the position co-ordinate  $x$ , the authors preferred to use the expression “mode” or “eigenfunction” as seldom as possible, unlike in Ref. [1]. Whenever necessary, those words were used in quotation marks.  $C_i(x)$  which is simply the absolute value of  $Z_i(x)$ , i.e.,  $\text{Abs}(Z_i(x))$ , represents the amplitude distribution over the  $i$ th step of the rod.

With the method given above, the eigenvalues  $\lambda$  of the axially vibrating multi-step rod are found as the roots of a complex determinant of size  $(2n \times 2n)$  if the rod under consideration consists of  $n$  portions (steps). In the following, an alternative form of the characteristic equation will be given which could be preferable for numerical calculations especially for large  $n$  values. The second

form is essentially a transfer matrix method, which also makes use of the separation of variables approach at the beginning. Li and his co-workers applied it in a series of papers successfully to the longitudinal vibrations of rods and rod systems with variable cross-sections [3–5].

Here, the cross-sections of the rod are assumed to be constant along a rod portion, but external viscous damping is allowed to act on the rod.

The axial displacement distribution along the  $i$ th portion of the rod given in Eq. (11) can be rewritten as

$$Z_i(x) = \bar{A}_i S_{i,1}(x) + \bar{B}_i S_{i,2}(x), \tag{22}$$

where the abbreviations

$$S_{i,1}(x) = e^{v_i x}, \quad S_{i,2}(x) = e^{-v_i x} \tag{23}$$

are introduced. Let us assume in what follows that  $x = 0$  corresponds to the left end of the  $i$ th rod portion. The results in Ref. [3] can be adopted appropriately.

The relationship between the parameters,  $Z_{i,1}$  (axial displacement) and  $N_{i,1}$  (axial force) at the right end (denoted by the subscript 1 in Fig. 1) and at the left end of the  $i$ th portion (subscript 0 in Fig. 1) can be expressed in matrix notations as

$$\begin{bmatrix} Z_{i,1} \\ N_{i,1} \end{bmatrix} = \mathbf{T}_i \begin{bmatrix} Z_{i,0} \\ N_{i,0} \end{bmatrix}, \tag{24}$$

in which

$$\mathbf{T}_i = \begin{bmatrix} S_{i,1}(L_i) & S_{i,2}(L_i) \\ k_i S'_{i,1}(L_i) & k_i S'_{i,2}(L_i) \end{bmatrix} \begin{bmatrix} S_{i,1}(0) & S_{i,2}(0) \\ k_i S'_{i,1}(0) & k_i S'_{i,2}(0) \end{bmatrix}^{-1} \quad (i = 1, \dots, n), \tag{25}$$

where a prime denotes derivative with respect to  $x$ . The matrix  $\mathbf{T}_i$  is called the transfer matrix because it transfers the parameters at the end 0 to those at the end 1 of the  $i$ th step rod. It can be shown that the transfer matrix transferring the parameters at the station 0 of the first rod step to the right end of the multi-step rod carrying the tip mass is

$$\mathbf{T} = \mathbf{T}_M \mathbf{T}_n \cdots \mathbf{T}_1 = \begin{bmatrix} T_{11} & T_{12} \\ T_{21} & T_{22} \end{bmatrix}, \tag{26}$$

where

$$\mathbf{T}_M = \begin{bmatrix} 1 & 0 \\ \lambda^2 M & 1 \end{bmatrix} \tag{27}$$

accounts for the tip mass.

In case of the system in Fig. 1, the boundary conditions are such that the axial displacement at the left end and the axial force at the right end of the multi-step rod system vanish. This leads to the characteristic equation

$$T_{22}(v_1(\lambda), \dots, v_n(\lambda)) = T_{22}(\lambda) = 0. \tag{28}$$

If there is no tip mass, the matrix  $\mathbf{T}_M$  reduces to the  $2 \times 2$  unit matrix. Hence, the overall transfer matrix  $\mathbf{T}$  reduces to the product of  $n$  sub-transfer matrices  $\mathbf{T}_i$ :

$$\mathbf{T} = \mathbf{T}_n \cdots \mathbf{T}_1. \quad (29)$$

The characteristic equation (28) holds formally where  $T_{22}$  denotes this time the (2,2) element of the matrix  $\mathbf{T}$  given in Eq. (29). In case the tip mass tends to infinity, i.e., the rod is fixed–fixed, the boundary conditions impose that the axial displacements at both ends of the multi-step rod vanish which leads to the characteristic equation

$$T_{12}(\lambda) = 0, \quad (30)$$

where the overall transfer matrix  $\mathbf{T}$  is given by Eq. (29).

### 3. Numerical evaluations

This section is devoted to the numerical evaluation of the expressions obtained above. The computation will be demonstrated using a three-step rod with the parameters given in Table 1.

Three cases are considered: In the first case, it is assumed that there is no tip mass, i.e.,  $M = 0$  (case I), in the second case, there is a tip mass:  $M \neq 0$  (case II) and finally, the tip mass is infinite, i.e., the three-step rod is fixed–fixed (case III). As can be seen from Table 1, in all cases, the physical parameters of the rod steps are equal. The tip mass in case II is ( $M =$ )50 kg.

Table 2 gives the “first” six eigenvalues of the system for case I. It is seen that the physical parameters lead to both overdamped and underdamped “modes”. The numerical values in the first column represent the results of finding the roots of the determinantal equation in Eq. (16), whereas those of the second column are results of Eq. (28) based on the transfer matrix method. This holds for Tables 3 and 4 also. The numbers in both columns are exactly the same. The upper parts of Fig. 2 shows for case I the three-dimensional plots of  $w_i(x, t)$  for the first three overdamped eigenvalues. In the lower part, the amplitude distribution  $\text{Abs}(Z_i(x))$  which is composed of  $n$  curves of  $\text{Abs}(Z_i(x))$  corresponding to  $n$  steps on the rod is plotted.

As in Fig. 2, the upper part of Fig. 3 shows for case I, the  $w_i(x, t)$ -surfaces for the “first” three underdamped eigenvalues. The lower part gives the amplitude distributions.

Table 3 gives the “first” six eigenvalues for case II. Again, both those of the overdamped and the underdamped “modes” are given. The numerical values in both columns are the same.

Figs. 4 and 5 are concerned with case II. As in Figs. 2 and 3, the upper parts of Figs. 4 and 5 reflect the  $w_i(x, t)$  plots of the “first” three overdamped and underdamped eigenvalues, respectively. The lower parts give again the corresponding amplitude distributions.

Finally, Table 4 collects the “first” six eigenvalues for case III, where the numerical values in both columns are the same, as previously. Figs. 6 and 7 are concerned with this case. As above, the upper parts of these figures give the  $w_i(x, t)$  plots of the “first” three overdamped and underdamped eigenvalues, respectively. The lower parts give the corresponding amplitude distributions.

Comparison of the overdamped eigenvalues in Tables 2 and 3 reveals that the attachment of the tip mass causes the eigenvalues to increase in absolute value and this increases the damping effect. In comparison to Table 3 (case II), the overdamped eigenvalues in Table 4 (case III) have greater

Table 1  
The physical parameters of the rods in cases I–III

	Step 1	Step 2	Step 3
$L_i$ (m)	1	2	2
$m_i$ (kg/m)	20	10	10
$c_i$ (kg/ms)	0	0	200
$E_i A_i$ (N)	200	100	50

Table 2  
The “lower” eigenvalues for case I

From Eq. (16)	From Eq. (28)
-0.06379	-0.06379
-0.85199	-0.85199
-3.59985	-3.59985
$-0.37373 \pm 3.22304i$	$-0.37373 \pm 3.22304i$
$-0.41517 \pm 5.76661i$	$-0.41517 \pm 5.76661i$
$-0.72281 \pm 9.02664i$	$-0.72281 \pm 9.02664i$

Table 3  
The “lower” eigenvalues for case II

From Eq. (16)	From Eq. (28)
-0.06452	-0.06452
-1.14637	-1.14637
-7.19848	-7.19848
$-0.83926 \pm 1.33153i$	$-0.83926 \pm 1.33153i$
$-0.37410 \pm 3.22334i$	$-0.37410 \pm 3.22334i$
$-0.41518 \pm 5.76657i$	$-0.41518 \pm 5.76657i$

absolute values. In other words, the eigenmotions of the fixed–fixed rod corresponding to these eigenvalues damp out more rapidly than in the case of the rod carrying a tip mass.

Comparison of the underdamped eigenvalues in Tables 2 and 3 shows that the (complex) “eigenfrequencies” of the axial vibrations are decreased due to the inclusion of the tip mass, as expected. Further, the comparison of numerical values in Tables 3 and 4 reveals that the “eigenfrequencies” in the fixed–fixed rod case are larger than in the case of a tip mass, because the system is stiffer.

Concerning the number of nodes, the behaviors of the three cases are similar for overdamped “modes”. As can be seen from the lower parts of Figs. 2, 4 and 6, the second and third “modes” reveal 1 and 2 nodes, respectively. Further, the nodes are located in the damped portion. On the contrary, underdamped “modes”, reveal no nodes as can be seen from Figs. 3, 5 and 7.

Table 4  
The “lower” eigenvalues for case III

From Eq. (16)	From Eq. (28)
-0.30937	-0.30937
-1.84783	-1.84783
-7.64425	-7.64425
$-0.37394 \pm 3.22334i$	$-0.37394 \pm 3.22334i$
$-0.41519 \pm 5.76658i$	$-0.41519 \pm 5.76658i$
$-0.72280 \pm 9.02662i$	$-0.72280 \pm 9.02662i$

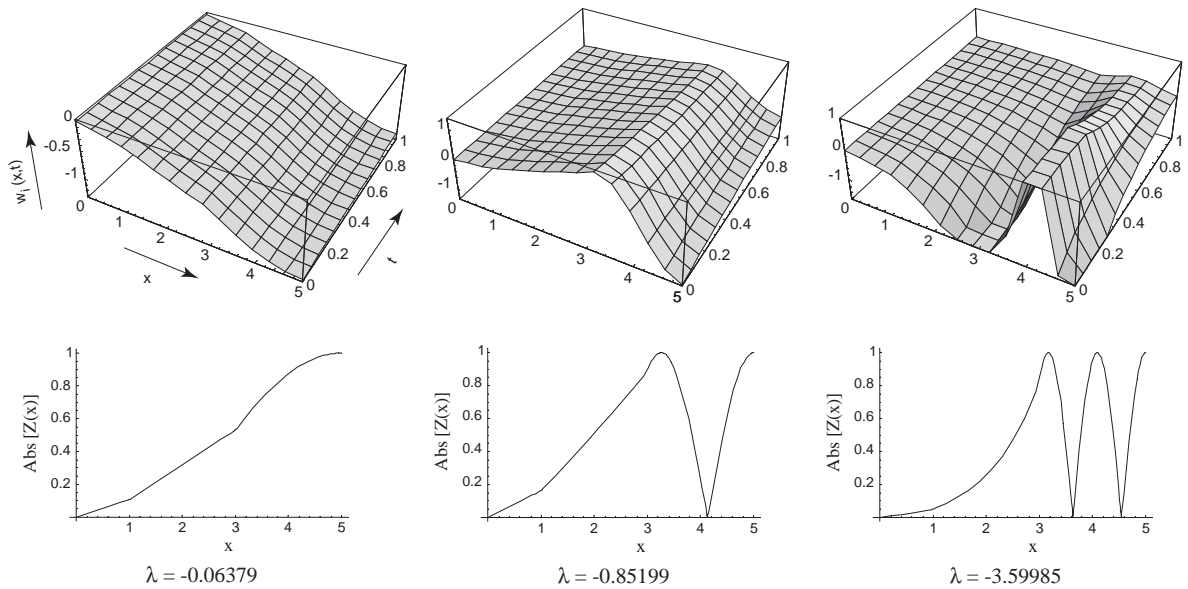


Fig. 2. Three-dimensional plots of  $w_i(x, t)$ -surfaces and amplitude distributions  $Abs(Z(x))$ , corresponding to the first three overdamped eigenvalues for case I.

In accordance with the fact that the third portion of the rod is damped and the first two are not, one observes that the majority of the displacements in the “lower” underdamped “modes” is local to the undamped, i.e., to the first two parts of the rod.

#### 4. Conclusions

This study is concerned with the establishment of two methods for computing the eigencharacteristics of a continuous rod, carrying a tip mass, consisting of several parts having different physical parameters and subjected to external viscous damping. Both methods use separation of variables approach at the beginning and differ, actually, in the solution of the



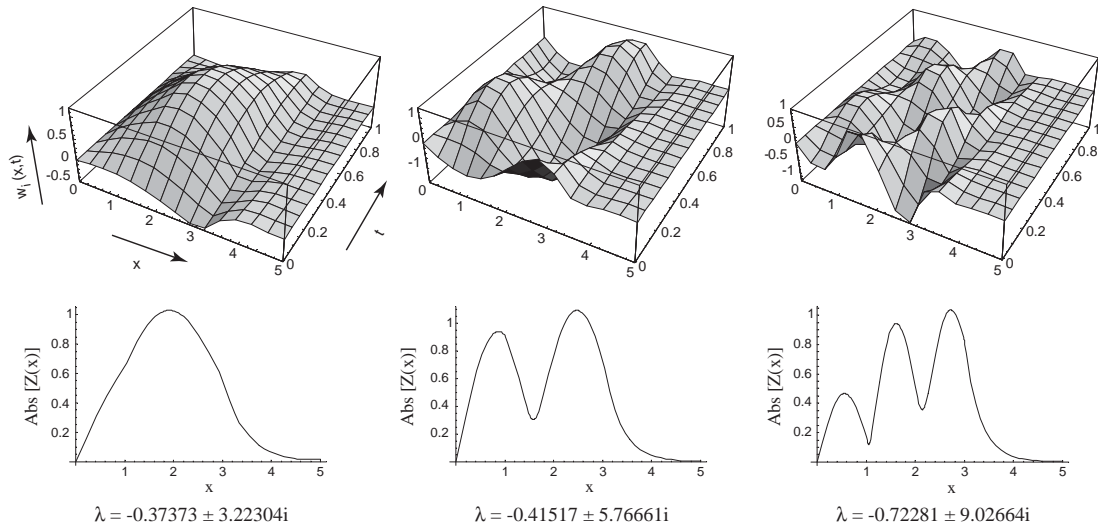


Fig. 3. Three-dimensional plots of  $w_i(x,t)$ -surfaces and amplitude distributions  $\text{Abs}(Z(x))$ , corresponding to the “first” three underdamped eigenvalues for case I.

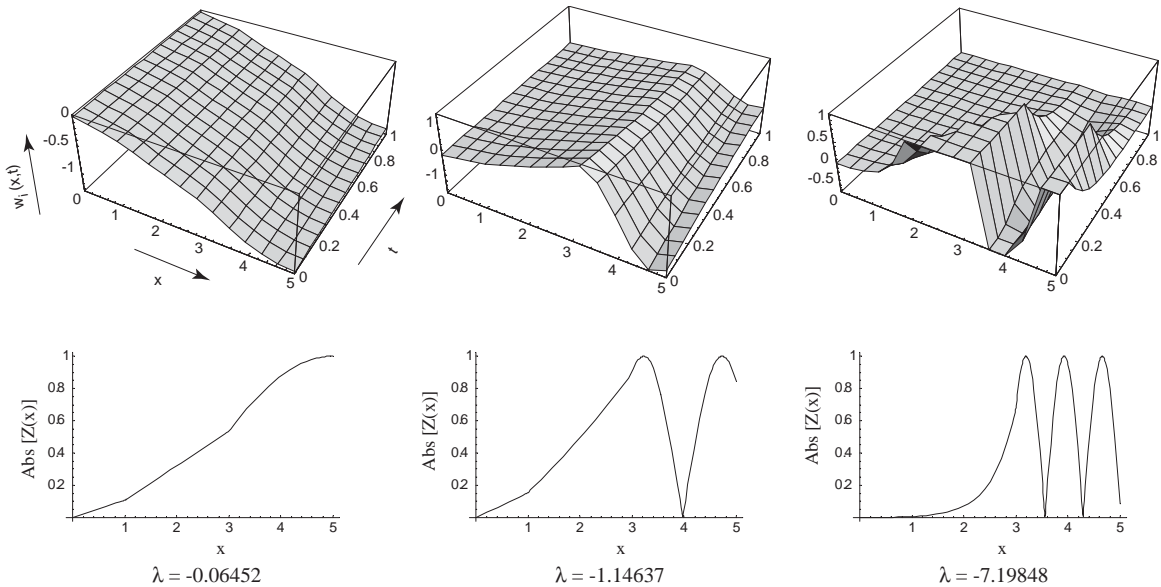


Fig. 4. Three-dimensional plots of  $w_i(x,t)$ -surfaces and amplitude distributions  $\text{Abs}(Z(x))$ , corresponding to the first three overdamped eigenvalues for case II.

corresponding ordinary differential equation. The second method is referred to as the transfer matrix method in the literature. Excellent agreement of the numerical results for three sample systems obtained via the two methods justifies the reliability of the formulae established.

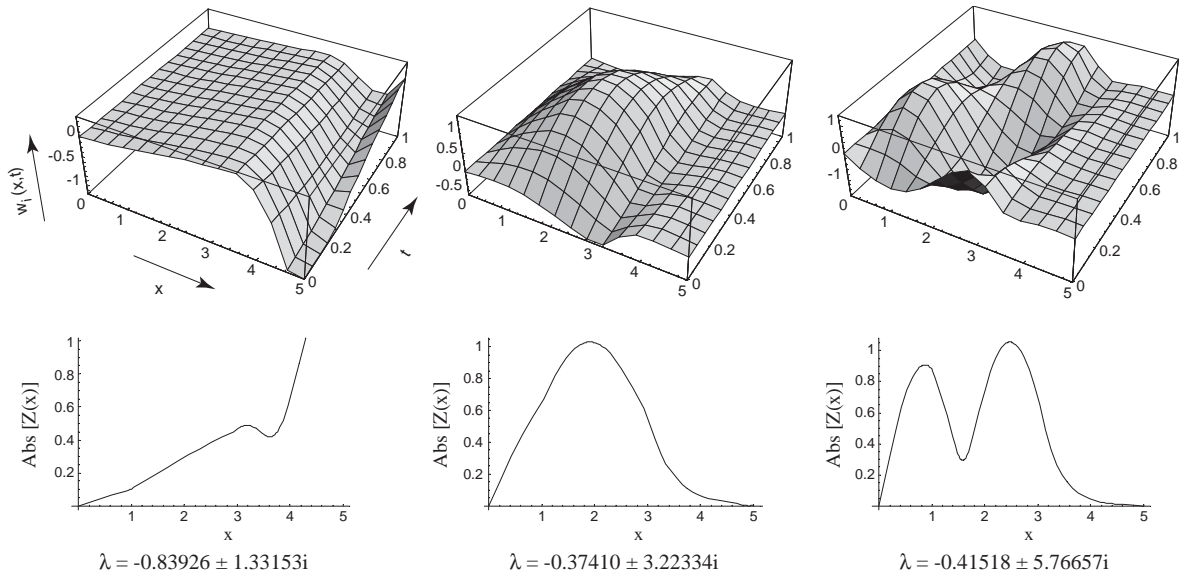


Fig. 5. Three-dimensional plots of  $w_i(x,t)$ -surfaces and amplitude distributions  $\text{Abs}(Z(x))$ , corresponding to the “first” three underdamped eigenvalues for case II.

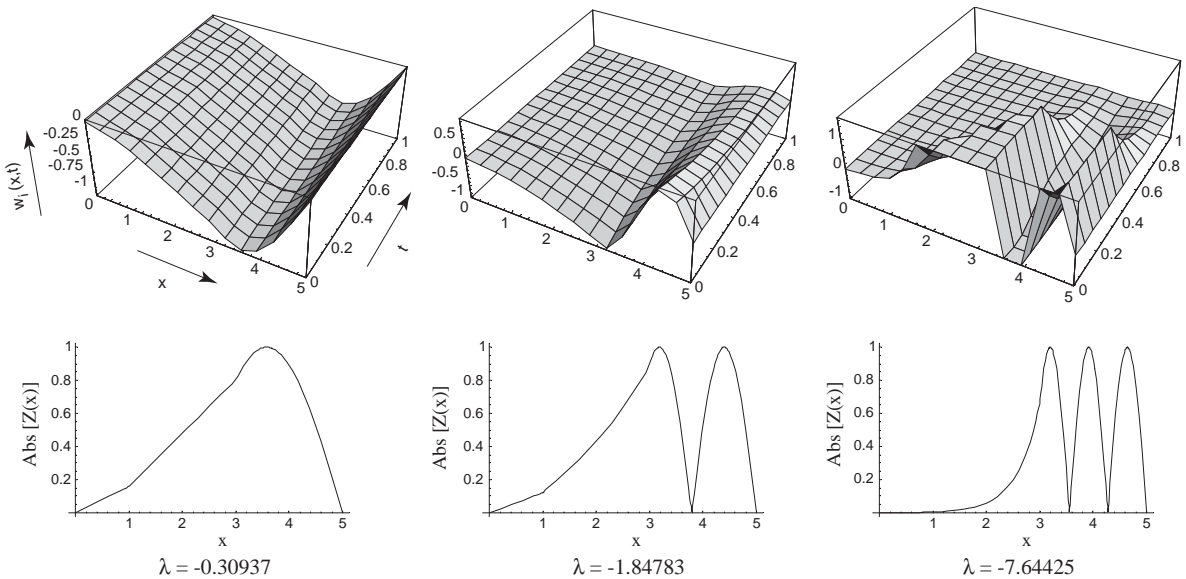


Fig. 6. Three-dimensional plots of  $w_i(x,t)$ -surfaces and amplitude distributions  $\text{Abs}(Z(x))$ , corresponding to the first three overdamped eigenvalues for case III.

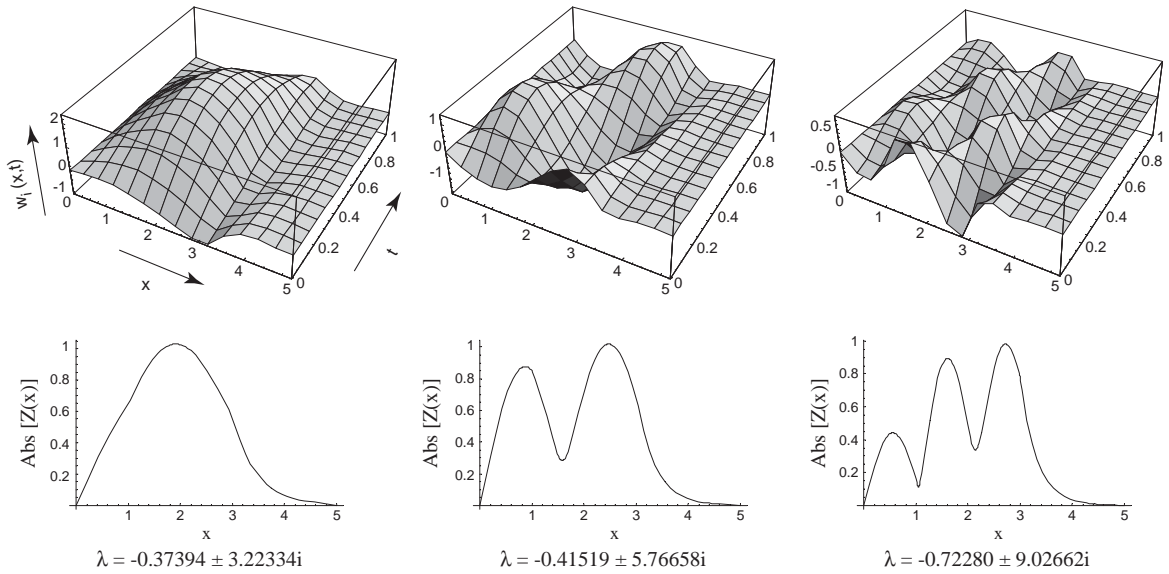


Fig. 7. Three-dimensional plots of  $w_i(x, t)$ -surfaces and amplitude distributions  $Abs(Z(x))$ , corresponding to the “first” three underdamped eigenvalues for case III.

**References**

[1] M.I. Friswell, A.W. Lees, The modes of non-homogeneous damped beams, *Journal of Sound and Vibration* 242 (2001) 355–361.

[2] M. Gürgöze, H. Erol, On the “modes” of non-homogeneously damped rods consisting of two parts, *Journal of Sound and Vibration* 260 (2003) 357–367.

[3] Q.S. Li, Exact solutions for longitudinal vibration of multi-step bars with varying cross-section, *Transactions of the American Society of Mechanical Engineers, Journal of Vibration and Acoustics* 122 (2000) 183–187.

[4] Q.S. Li, Exact solutions for free longitudinal vibrations of non-uniform rods, *Journal of Sound and Vibration* 234 (2000) 1–19.

[5] Q.S. Li, G.Q. Li, D.K. Liu, Exact solutions for longitudinal vibration of rods coupled by translational springs, *International Journal of Mechanical Sciences* 42 (2000) 1135–1152.